

Baryon resonances in asymmetric nuclear matter:

Implications for nuclear structure and astrophysics

J. Benlliure

University of Santiago de Compostela, Spain

NUSTAR Week

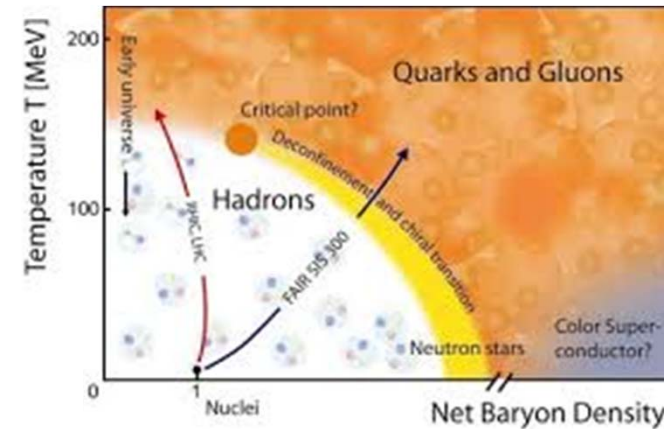
York, UK, September 26-30 2016

Subnucleonic degrees of freedom in nuclear matter

Compressed baryon matter.

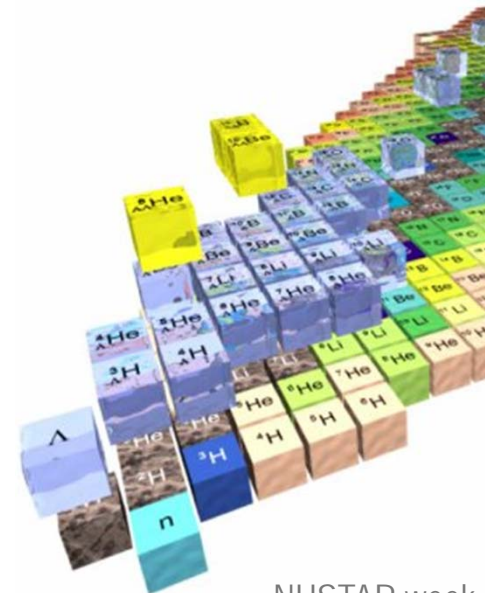
- ✓ Equation of State.
- ✓ Quark-gluon plasma.
- ✓ Neutron stars

Experimental investigation: relativistic heavy-ion collisions with stable nuclei



Exotic baryon matter.

- ✓ Isospin asymmetric nuclear matter
- ✓ Strange nuclear matter: hypernuclei
- ✓ Baryon resonance matter (ΔN , $N^* N$,.)



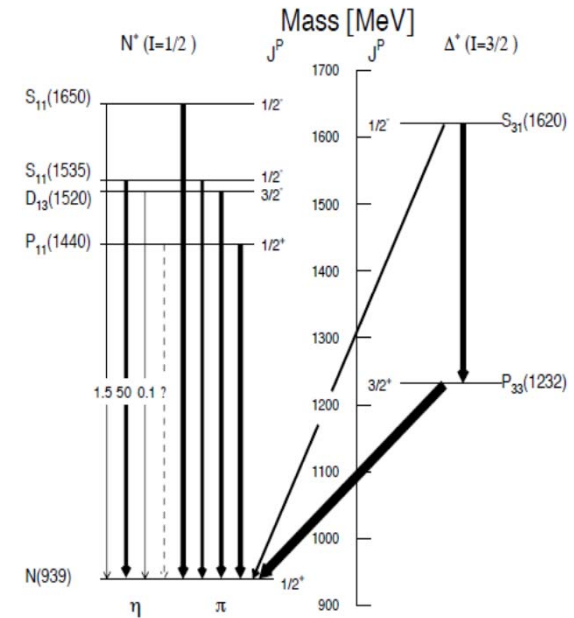
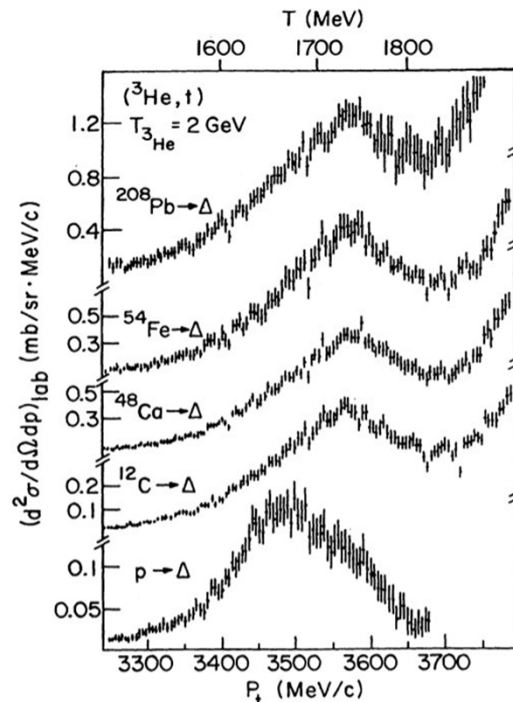
Subnucleonic degrees of freedom in nuclear matter

Baryon resonance matter.

- ✓ Nucleons in $I=1/2$ (N^*) and $I=3/2$ (Δ) excited states.
- ✓ Investigate ΔN , N^*N interactions (in-medium properties of the resonances)



baryon resonance matter



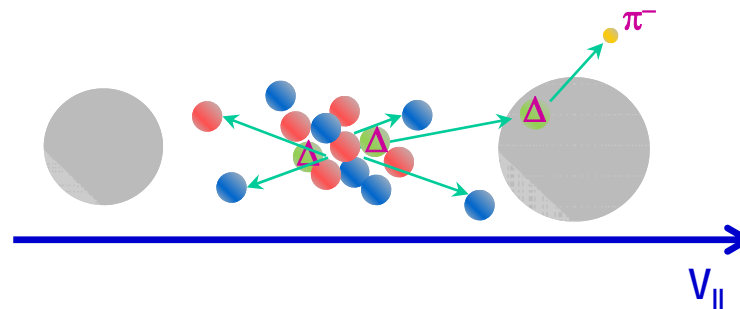
- ✓ A downward shift of about 70 MeV in the mass of the Delta resonance was observed in heavy ion collisions.
- ✓ No experimental information on baryon resonances in asymmetric nuclear matter

Outline

- ✓ Producing baryon resonance matter.
- ✓ Physics cases.
- ✓ Recent measurements at FRS@GSI.
experimental requirements
- ✓ First model calculations.
characterization of nucleon resonances
probing the neutron-proton abundance at the nuclear periphery
- ✓ Future perspectives at FAIR

Baryon resonance nuclei

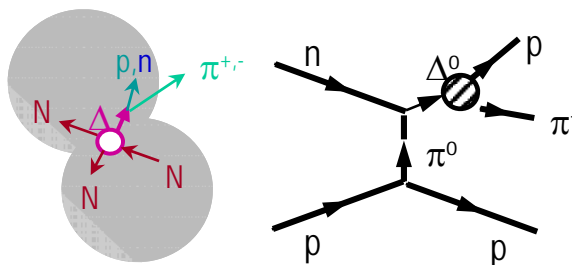
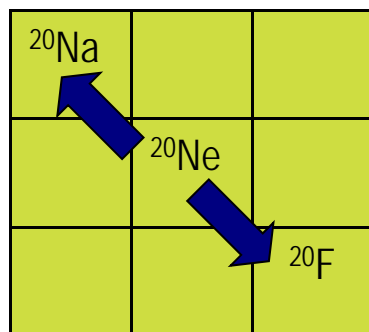
Nuclei with excited subnucleonic states can only be produced in collisions at energies above the pion production threshold ~ 300 MeV.



- ✓ Baryon resonances are produced in NN collisions in the participant zone at mid-rapidity
- ✓ Eventually some of these resonances are produced with a velocity compatible with the velocity of the projectile remnant nucleons and gets attached.
- ✓ These short lived states decays by emitting pions.
- ✓ In-medium ΔN or N^*N interactions can be characterized by determining the mass and width of the resonance

Isobar charge-exchange reactions

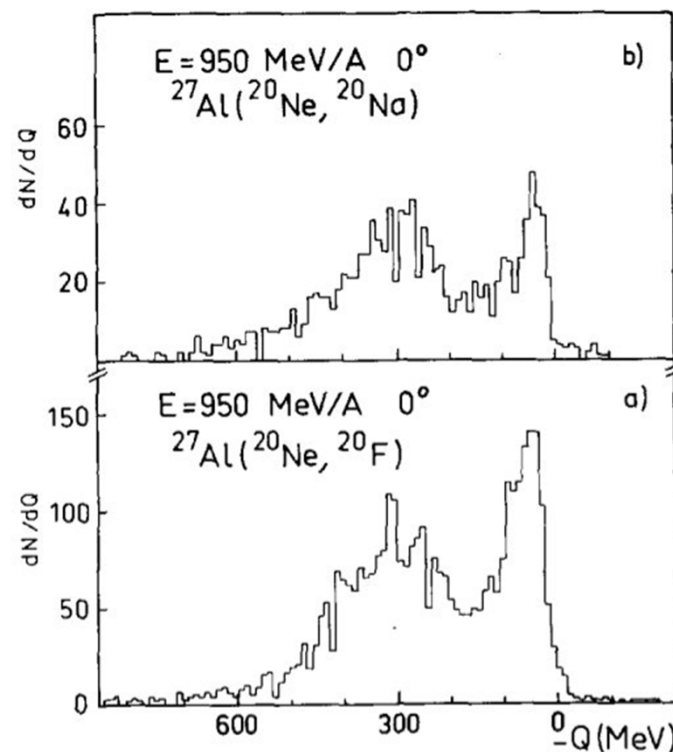
Isobar charge-exchange reactions investigated in inverse kinematics allow for the direct observation of in-medium excitation of the baryon resonances for both (p,n) and (n,p) channels.



The only missing particle: pion (to preserve the isobar character of the reaction).

- ✓ Clean reaction mechanism.
- ✓ Surface process (low density).
- ✓ Applicable with RIBs

C. Bachelier et al. PLB 172 (1986) 23



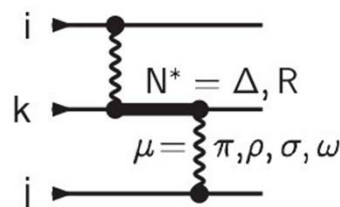
The momentum recoil induced by the pion emission proves the excitation of the resonance.

Physics cases

Baryon resonances in ground-state and structural properties of nuclei.

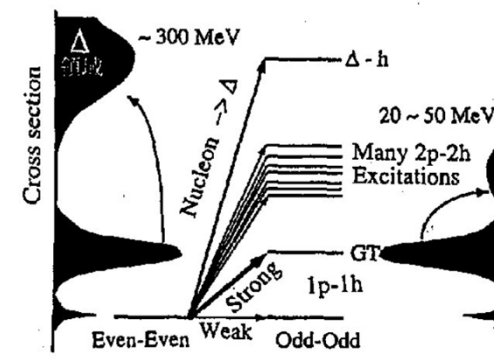
- ✓ Three-body nuclear forces.

role of $\Delta(1232)$ and $N^*(1440)$



- ✓ Gamow-Teller strength quenching.

role of Δ -h excitations



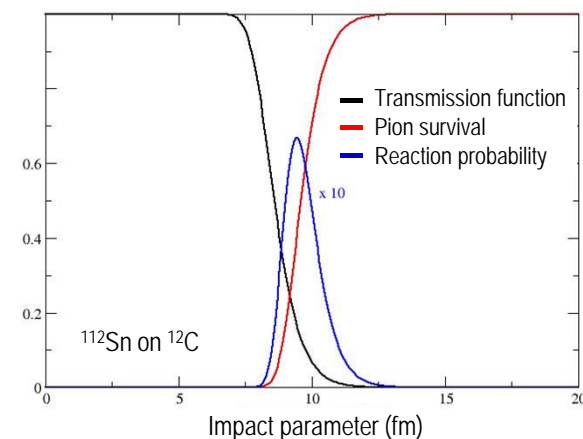
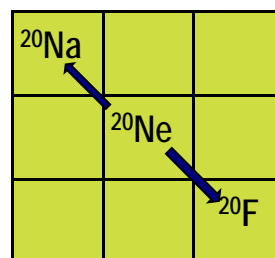
- ✓ Probing the neutron/proton content at the nuclear periphery.

symmetry energy

Isobar charge-exchange reactions are surface dominated:

(n,p) probability sensitive to neutron abundance

(p,n) probability sensitive to proton abundance



Physics cases

Baryon resonances and EoS

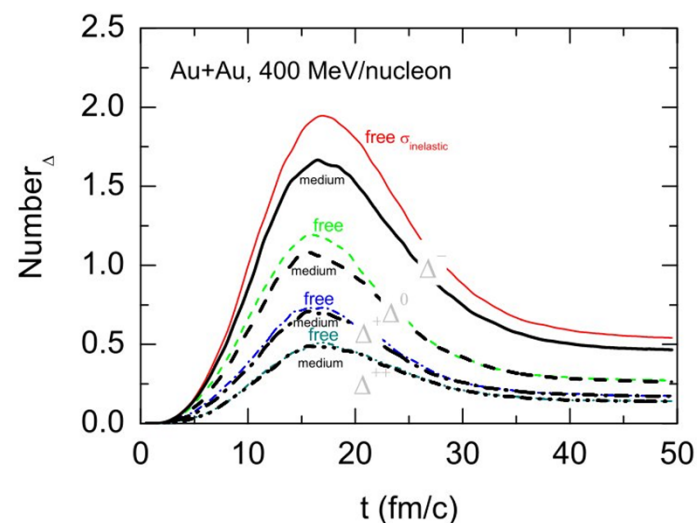
- ✓ The Δ isobar dynamics in transport models.

In-medium mass shift?

Δ potential and pion and kaon production

Bao-An Li PRC 92, 034603 (2015)

G. Yong et al.. PRC 92, 044610 (2016)

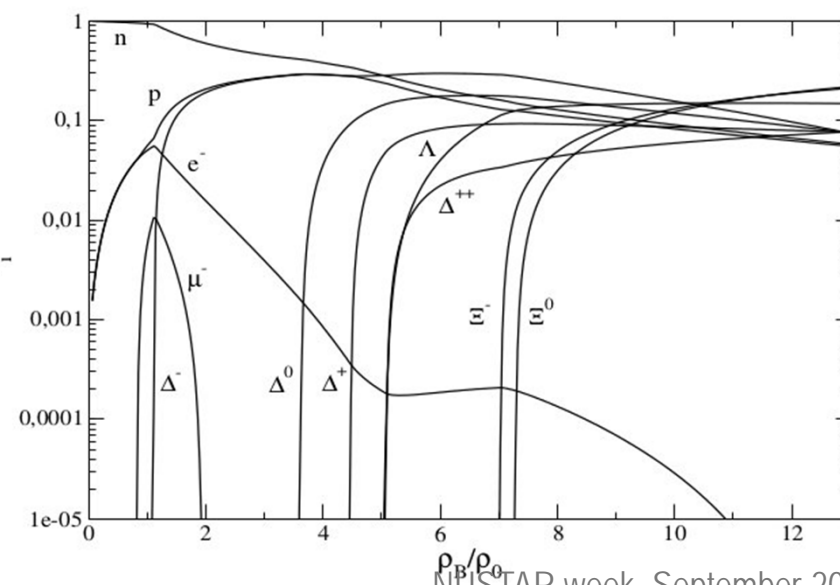


- ✓ Role of nucleon excitations in compact and massive neutron stars.

Recent constraints of the symmetry energy ($40 < L < 62$ MeV), make Δ isobars appear at $2-3 \rho_0$ softening neutron star EoS, the « Δ puzzle».

A. Drago et al.. PRC 90, 065809 (2014)

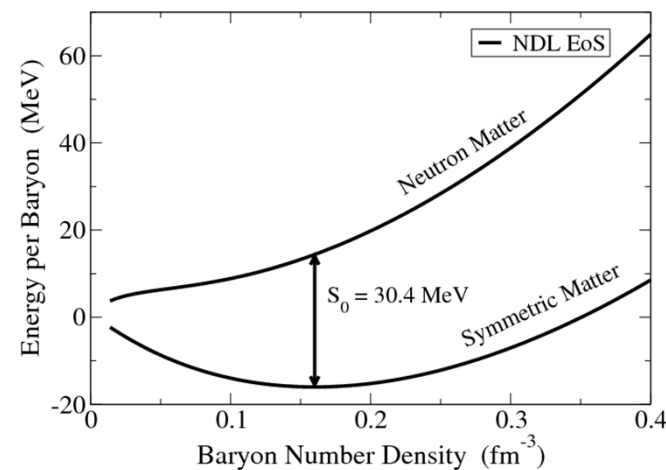
B. Cai et al., PRC 92, 015802 (2015)



Physics cases

Probing the ΔN potential with density and isospin asymmetry

Central collisions induced by relativistic radioactive nuclear beams.



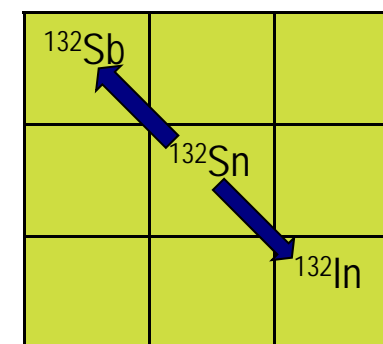
- ✓ No conclusive results on (p, π) invariant masses in stable heavy-ion collisions .
- ✓ No available information on the isovector component of the Δ potential.

Isobar charge-exchange reactions could represent a first step forward.

Experimental requirements

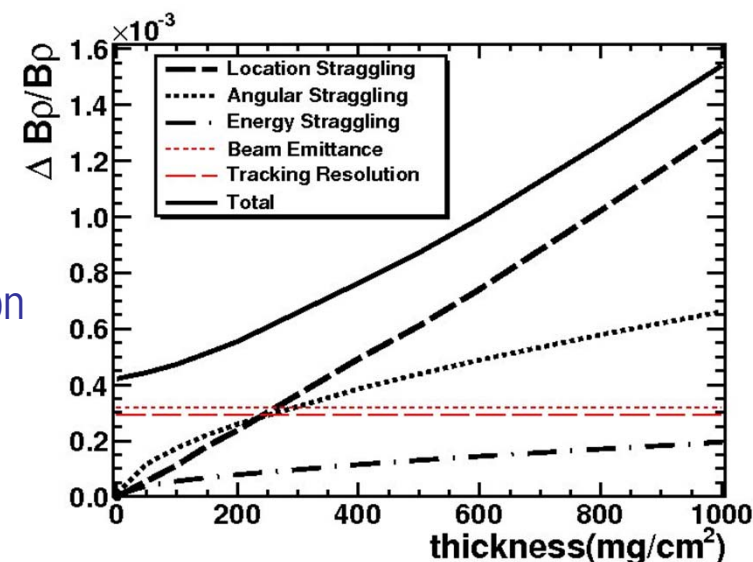
Observables:

- ✓ cross sections for both charge exchange reactions and channels
- ✓ missing-energy spectra
mean energy and width of the Δ -resonance



Requirements for the setup:

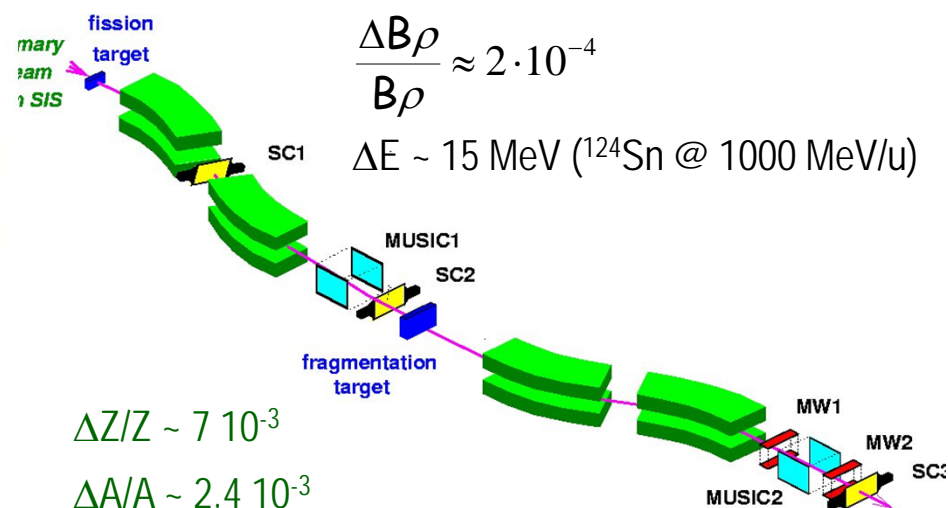
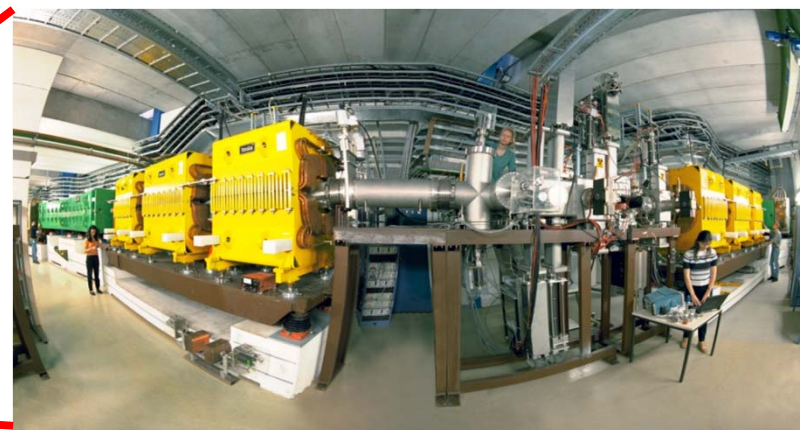
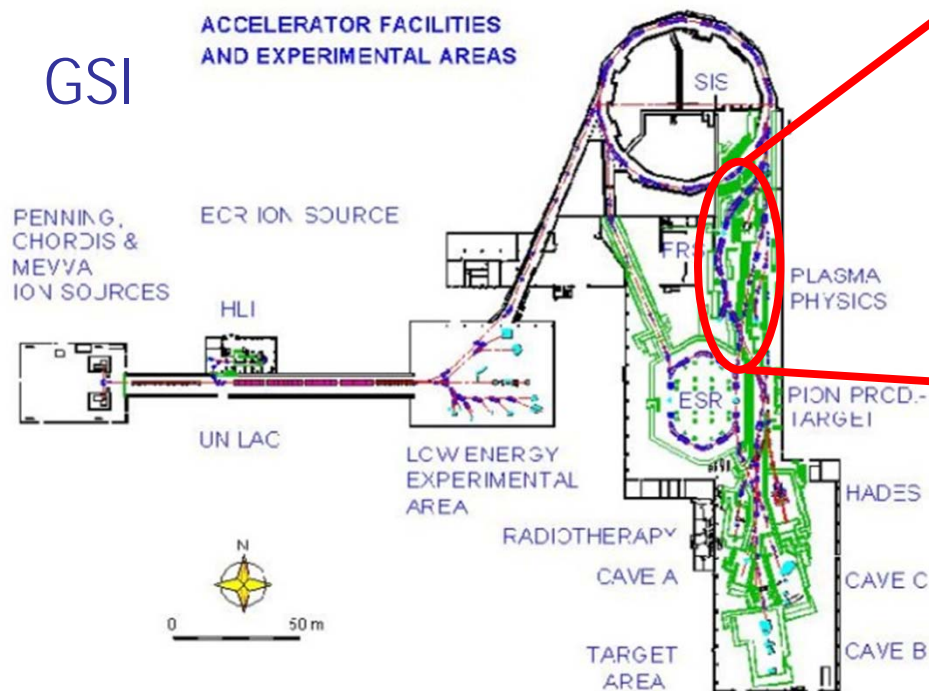
- ✓ isotopic identification of reaction ejectiles
- ✓ precise determination of the energy lost in the reaction
magnetic analysis of the reaction ejectiles
- ✓ best possible resolution.
improved position resolution and minimum matter



An exploratory experiment at GSI

Inverse kinematics

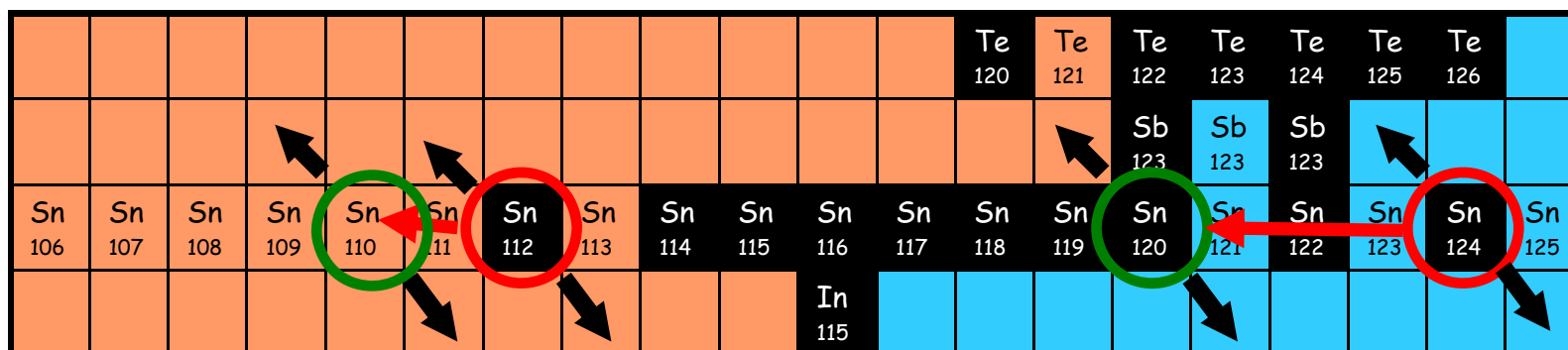
GSI



José Benlliure

An exploratory experiment

To investigate the feasibility of accurate measurements of nucleon resonances excited in isobar charge-exchange reactions induced by stable and unstable projectiles using the inverse kinematic technique.

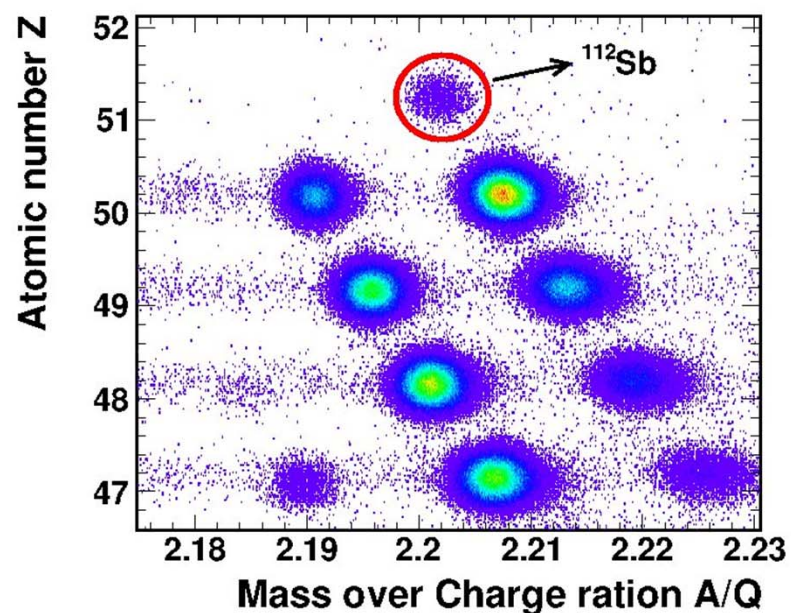


- ✓ $^{124}\text{Sn} + \text{CH}_2\text{C} \rightarrow ^{124}\text{Sb}, ^{124}\text{In} @ 1000 \text{ A MeV}$
- ✓ $^{124}\text{Sn} + \text{Be} \rightarrow ^{120}\text{Sn} + \text{CH}_2\text{C} \rightarrow ^{120}\text{Sb}, ^{120}\text{In} @ 1000 \text{ A MeV}$
- ✓ $^{112}\text{Sn} + \text{CH}_2\text{C}, \text{Cu}, \text{Pb} \rightarrow ^{112}\text{Sb}, ^{112}\text{In} @ 400, 700, 1000 \text{ A MeV}$
- ✓ $^{112}\text{Sn} + \text{Be} \rightarrow ^{110}\text{Sn} + \text{CH}_2\text{C} \rightarrow ^{110}\text{Sb}, ^{110}\text{In} @ 1000 \text{ A MeV}$

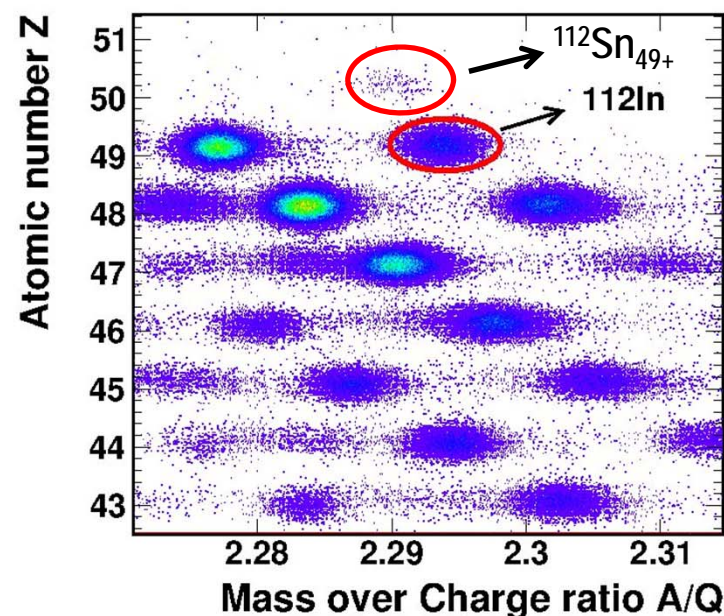
Recent measurements with the FRS

Isotopic identification of isobaric charge-exchange residues

$^{12}\text{C}(^{112}\text{Sn}, ^{112}\text{Sb})\text{X}$

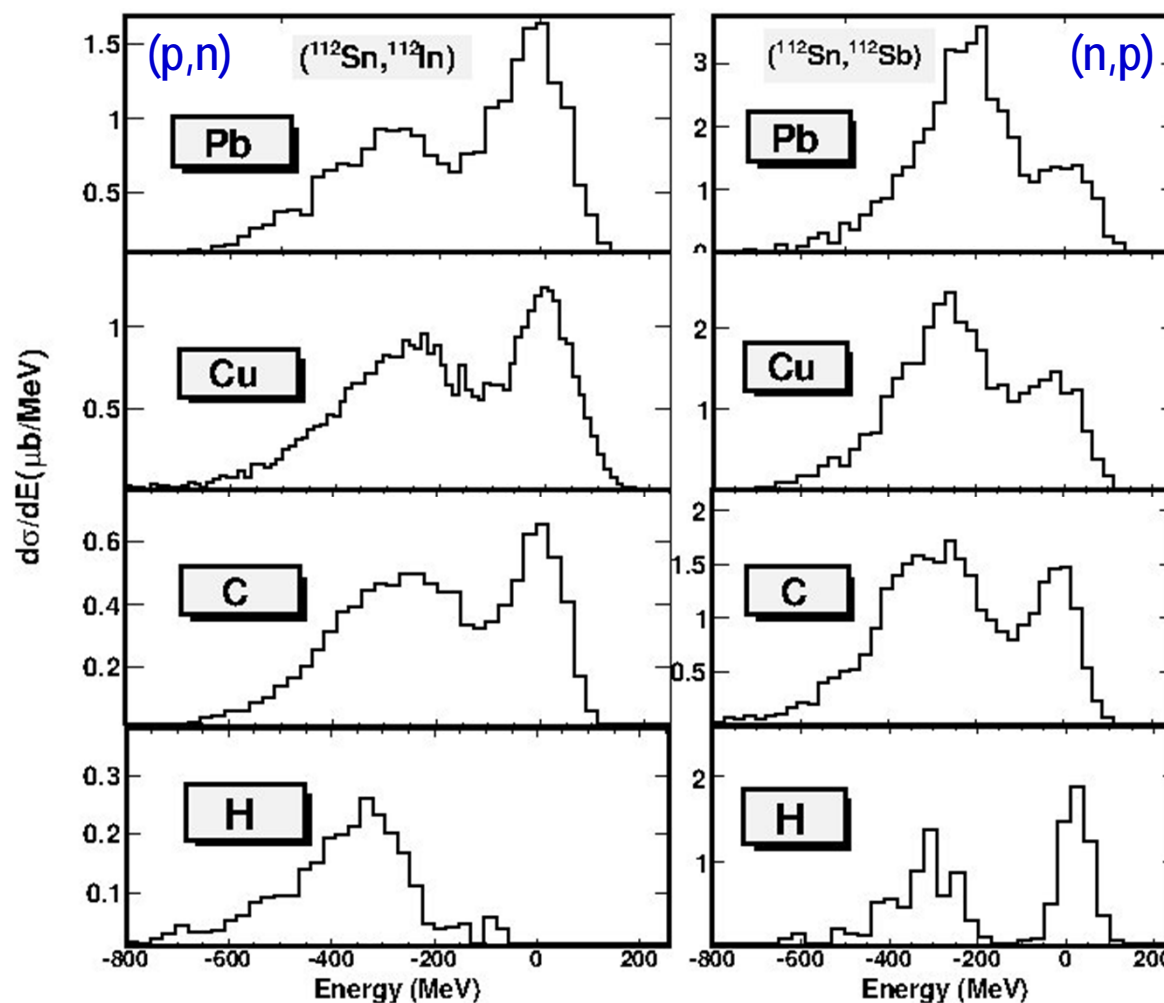


$^{12}\text{C}(^{112}\text{Sn}, ^{112}\text{In})\text{X}$



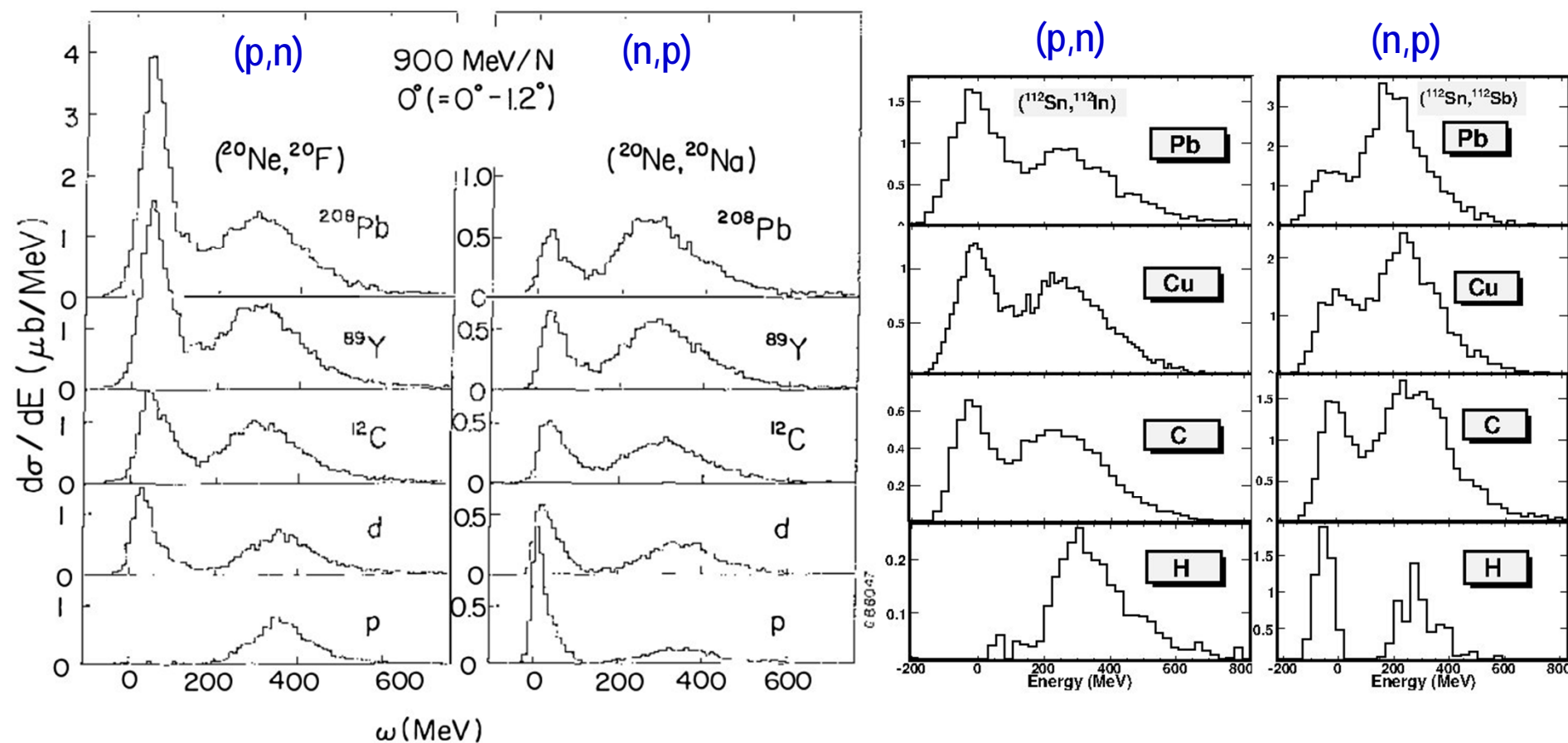
Recent measurements with the FRS

Missing-energy spectra in isobar charge-changing reactions induced by ^{112}Sn



Recent measurements with the FRS

Comparison with the Saturne data

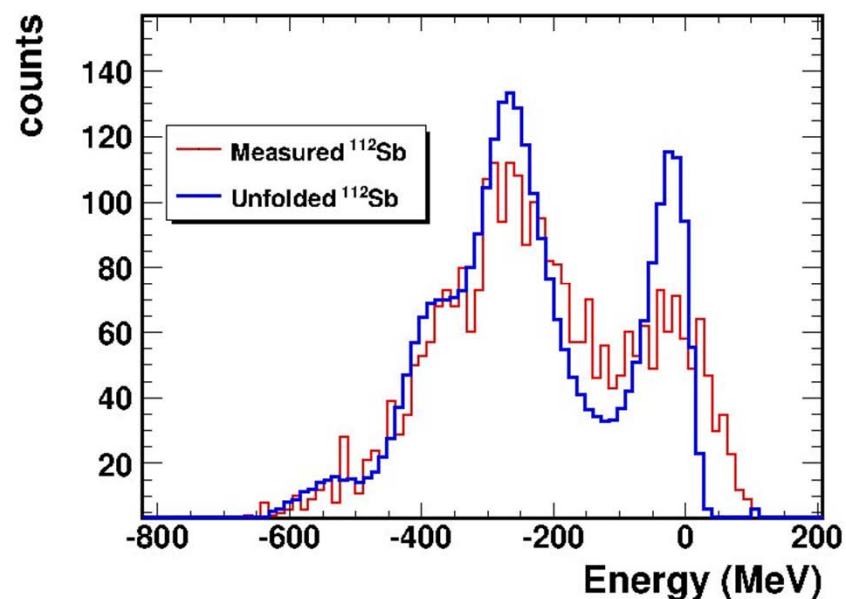
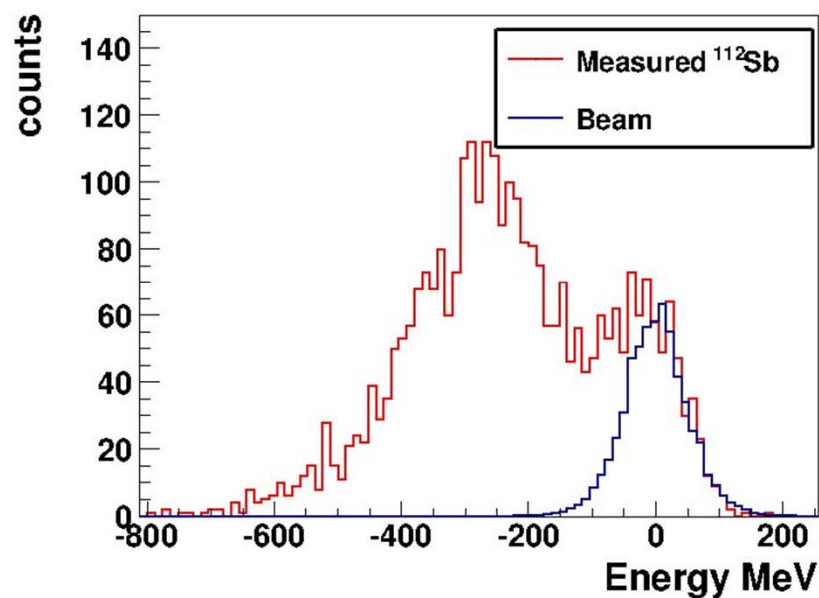


C. Bachellier et al. PLB 172 (1986) 23

Recent measurements with the FRS

Unfolding the missing-energy with the experimental response function

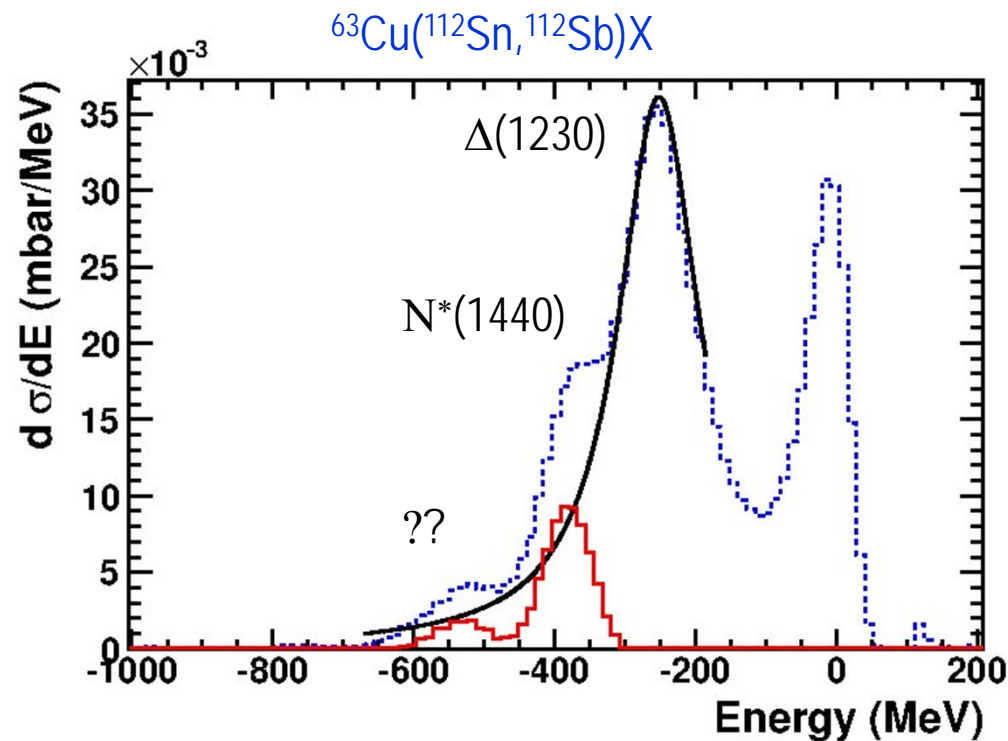
$^{63}\text{Cu}(^{112}\text{Sn}, ^{112}\text{Sb})X$



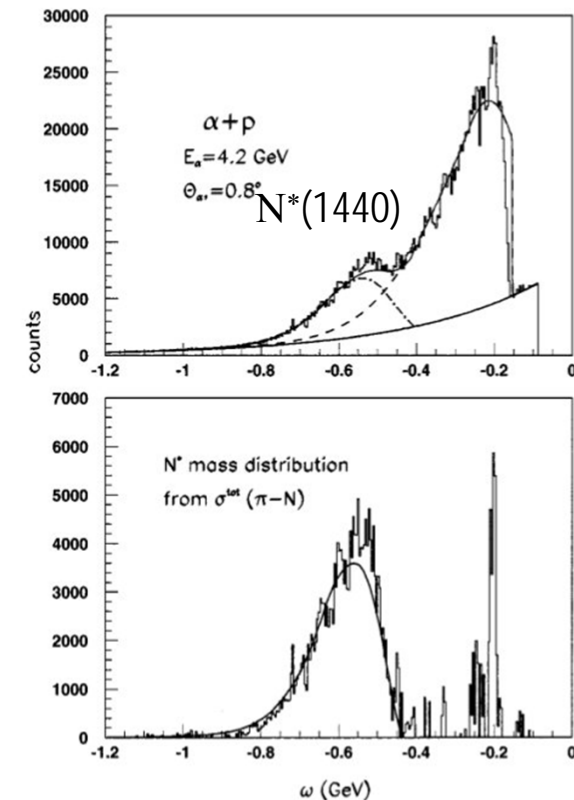
Final resolution after deconvolution $\Delta E \sim 15$ MeV ($^{124}\text{Sn}, ^{112}\text{Sn}$ @ 1000 A MeV)

Recent measurements with the FRS

Excitation of nucleon resonances



$p(\alpha, \alpha')X$ @ 4.2 GeV

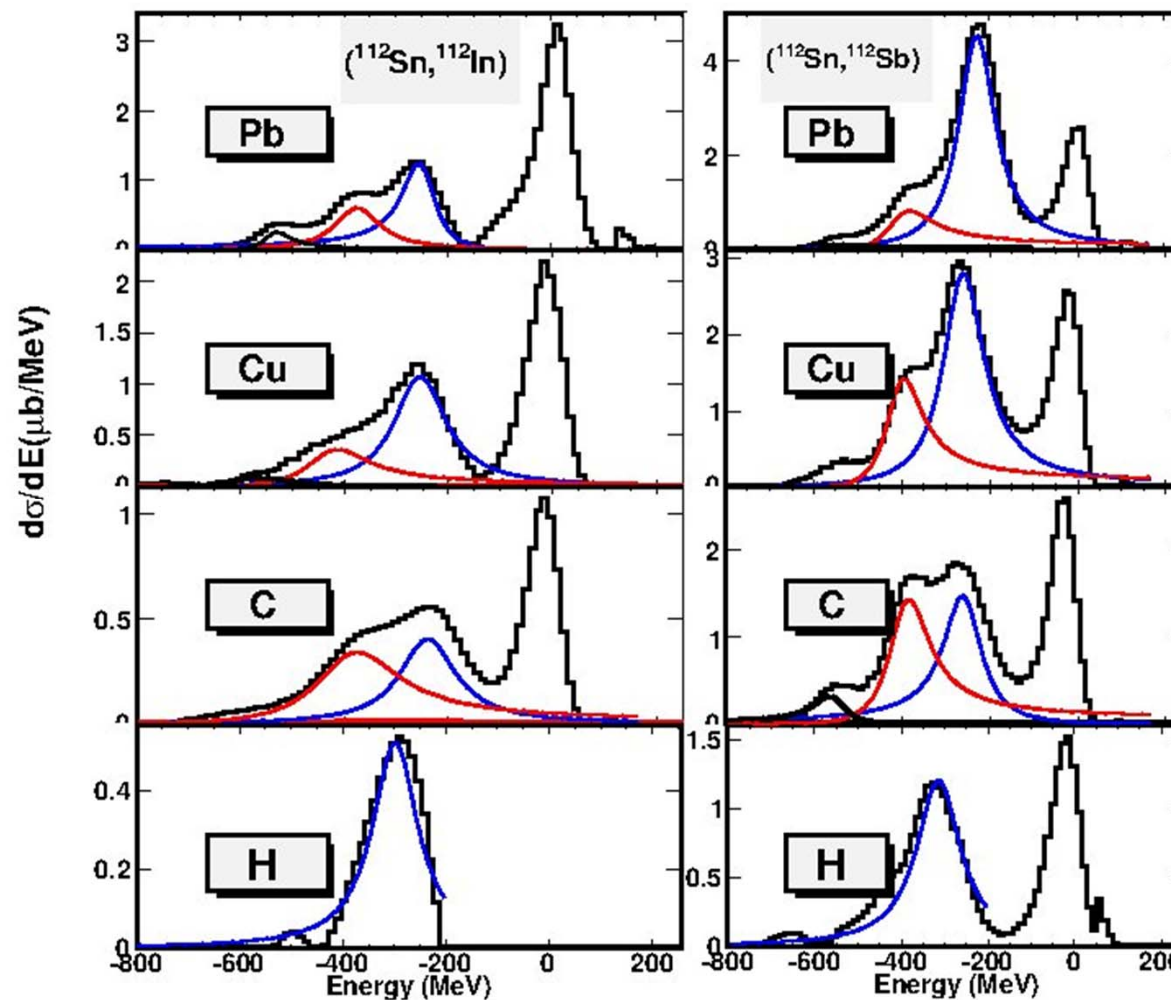


H.P. Morsch et al., PRL 69, 1336 (1992)

- ✓ The unfolded data show clear structures in the inelastic component
- ✓ The second substructure is tentatively identified as the Roper resonance

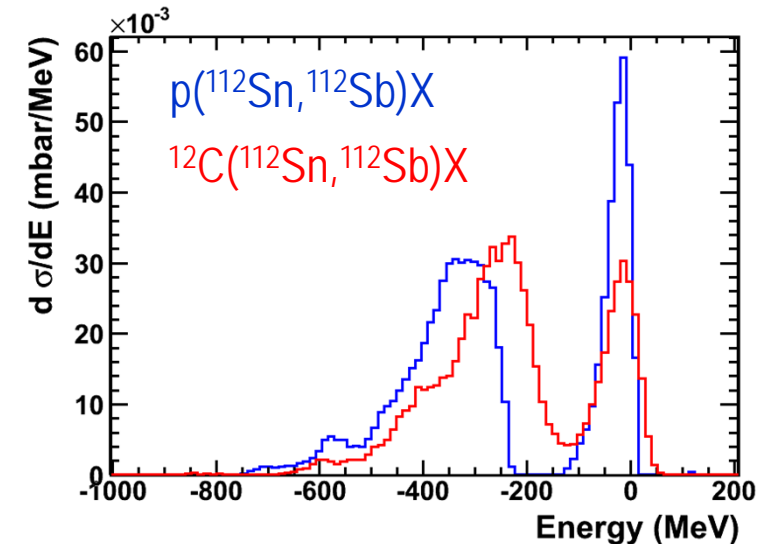
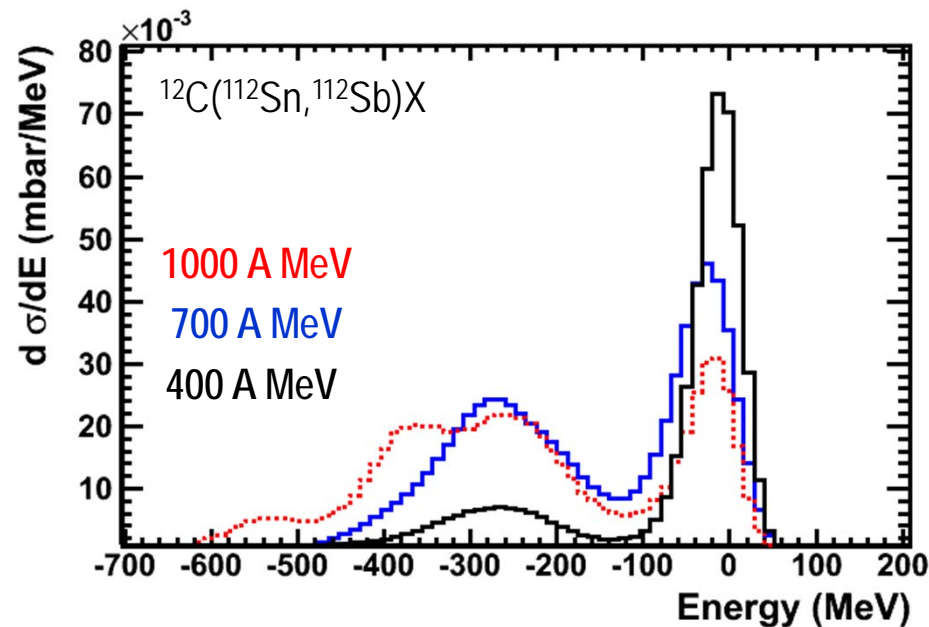
Recent measurements with the FRS

Unfolding the missing-energy with the experimental response function



Recent measurements with the FRS

Isobar charge-exchange reactions at relativistic energies

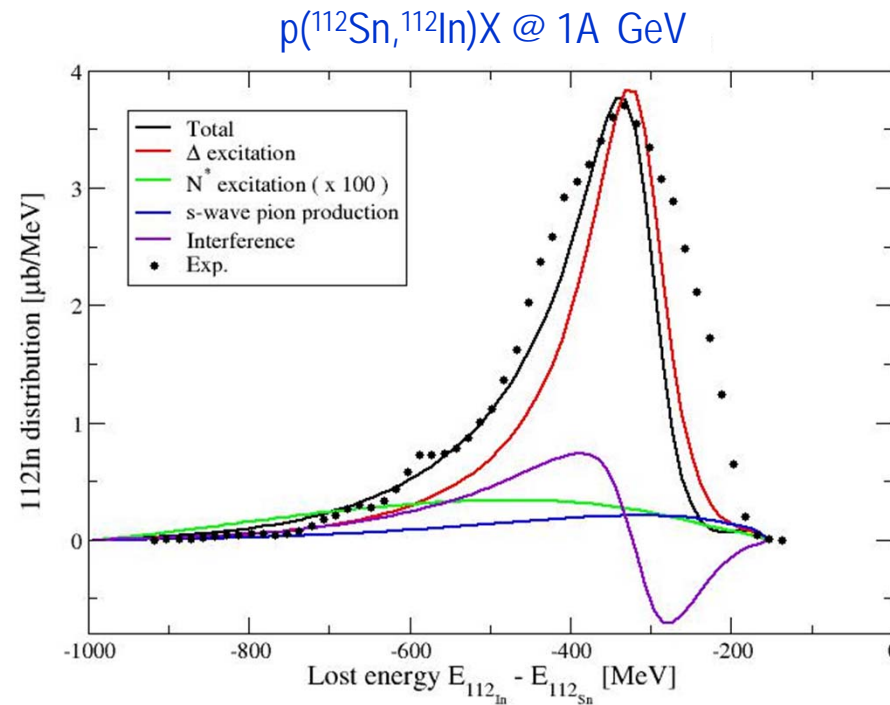


- ✓ The excitation probability of the resonances scales with energy as expected
- ✓ A downward shift in the energy of the resonances is also observed with composite targets

Characterization of in-medium baryon resonances

Benchmarking with isobar charge-exchange reactions:

Preliminary calculations, I. Vidaña

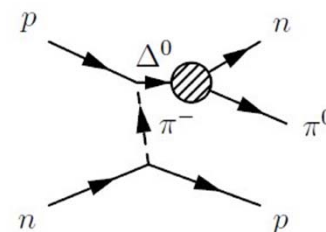
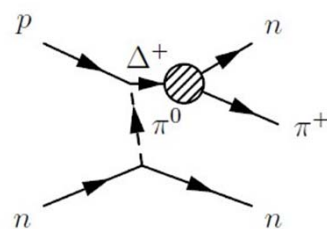
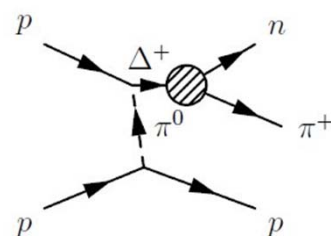


- ✓ The resonance properties used to describe elementary processes do not fully describe the in-medium production. Different in-medium coupling strengths ?....work on progress.

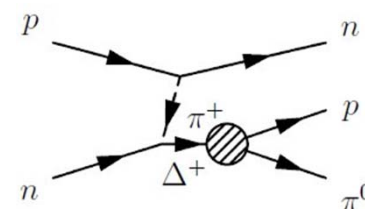
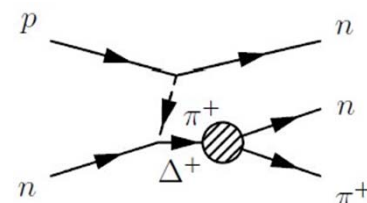
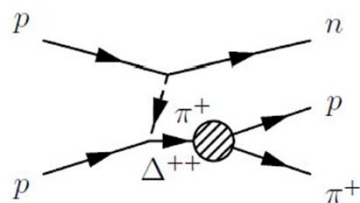
Characterization of in-medium baryon resonances

Projectile and target resonance excitations:

Projectile
excitations



Target
excitations

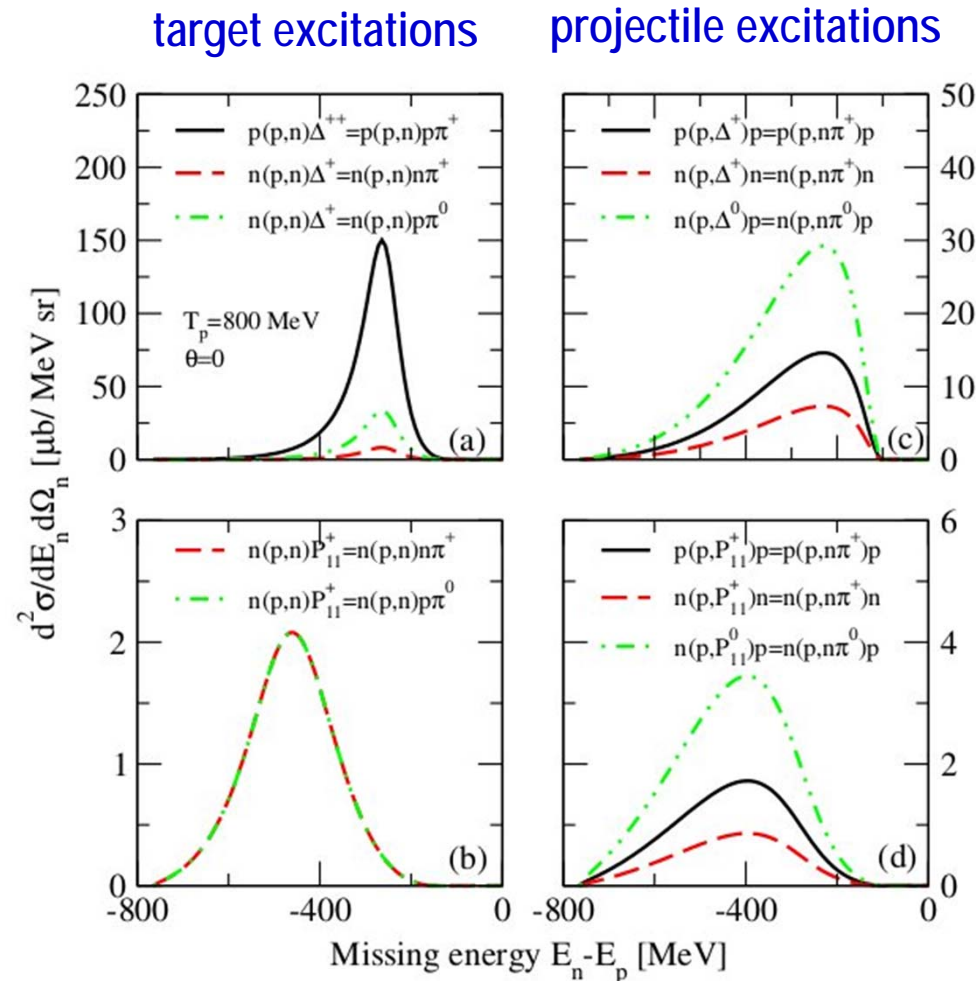


Baryon excitations in the projectile or target nucleus produced a similar effect in the missing energy spectra.

Characterization of in-medium baryon resonances

Projectile and target resonance excitations:

Isaac Vidaña, U. Coimbra



✓ The kinematical conditions of the pions emitted by the projectile or target nucleus produced missing energy spectra with a different shape affecting the apparent mean energy and width.

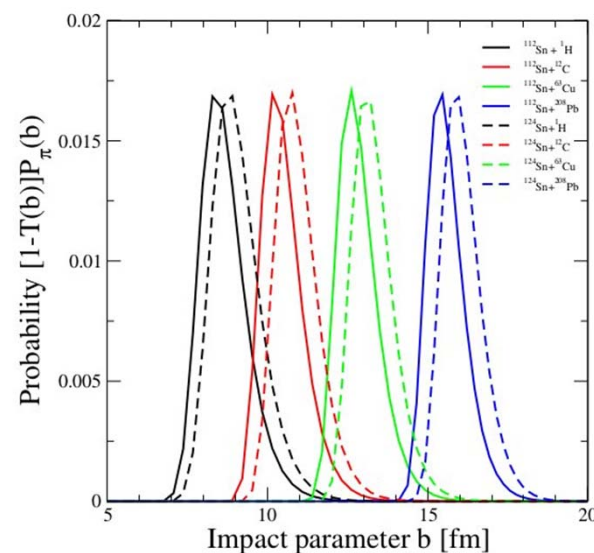
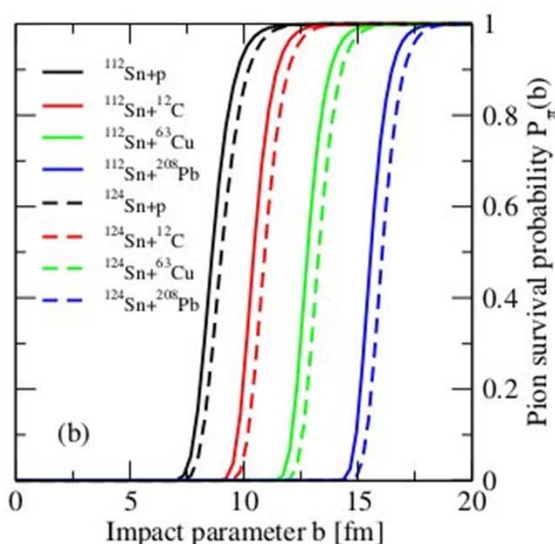
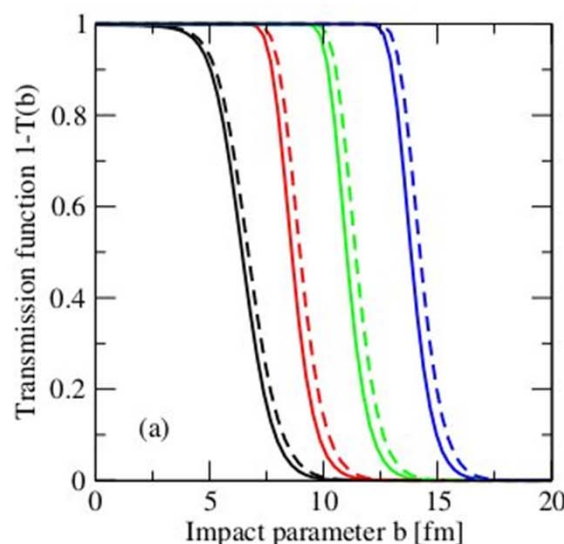
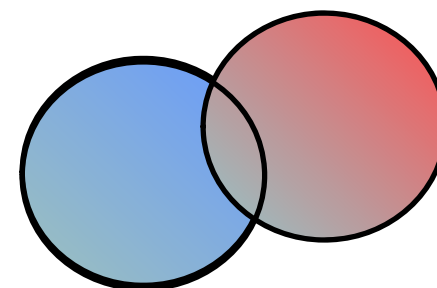
✓ Exclusive measurements tagging pions will help in separating both contributions.

Proton/neutron abundance at the nuclear surface

Charge-exchange cross sections

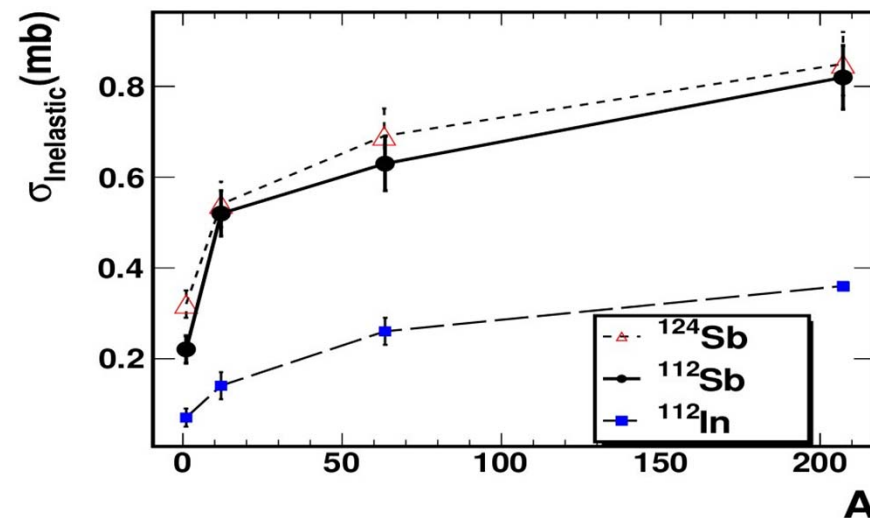
$$\left. \frac{d^2\sigma}{dE d\Omega} \right|_{(AZ, A(Z\pm 1))} = \sum_{N_2=n,p} \sum_{c=qe, in} \left(\frac{d^2\sigma}{dE_3 d\Omega_3} \right)_c N_{N_1 N_2}$$

$$N_{N_1 N_2} = \int d^2\vec{b} \rho_{overlap}^{N_1 N_2}(b) [1 - T(b)] P_\pi(b)$$



Proton/neutron abundance at the surface

Charge-exchange cross sections



- ✓ Cross sections are sensitive to the neutron excess at projectile periphery $\sigma(n,p) > \sigma(p,n)$ and the projectile size $\sigma(^{124}\text{Sb}) > \sigma(^{112}\text{Sb})$
- ✓ Simple targets such as protons or carbons seem better suited to link these cross sections to the relative abundance of protons and neutrons at the projectile periphery

Proton/neutron abundance at the nuclear surface

Ratio between isobaric charge-exchange channels

(n,p) $\Delta(1232)$ excitation

Excitation in the Target

$$\cancel{p(n,p)\Delta^0} - \cancel{p(n,p)n\pi^0} \quad (2/3)$$

$$\cancel{p(n,p)\Delta^0} - \cancel{p(n,p)p\pi^-} \quad (-\sqrt{2}/3)$$

$$\cancel{p(n,p)\Delta^-} - \cancel{p(n,p)n\pi^-} \quad (-\sqrt{2})$$

Excitation in the Projectile

$$p(n,\Delta^0)p = p(n,p\pi^-)p \quad (-\sqrt{2}/3)$$

$$\cancel{p(n,\Delta^+)n} - \cancel{p(n,p\pi^0)n} \quad (-2/3)$$

$$\cancel{n(n,\Delta^0)n} - \cancel{n(n,p\pi^-)n} \quad (\sqrt{2}/3)$$

(p,n) $\Delta(1232)$ excitation

Excitation in the Target

$$\cancel{p(p,n)\Delta^{++}} - \cancel{p(p,n)p\pi^+} \quad (\sqrt{2})$$

$$\cancel{n(p,n)\Delta^+} - \cancel{n(p,n)n\pi^+} \quad (\sqrt{2}/3)$$

$$\cancel{n(p,n)\Delta^+} - \cancel{n(p,n)p\pi^0} \quad (-2/3)$$

Excitation in the Projectile

$$p(p,\Delta^+)p = p(p,n\pi^+)p \quad (-\sqrt{2}/3)$$

$$\cancel{n(p,\Delta^+)n} - \cancel{n(p,n\pi^+)n} \quad (\sqrt{2}/3)$$

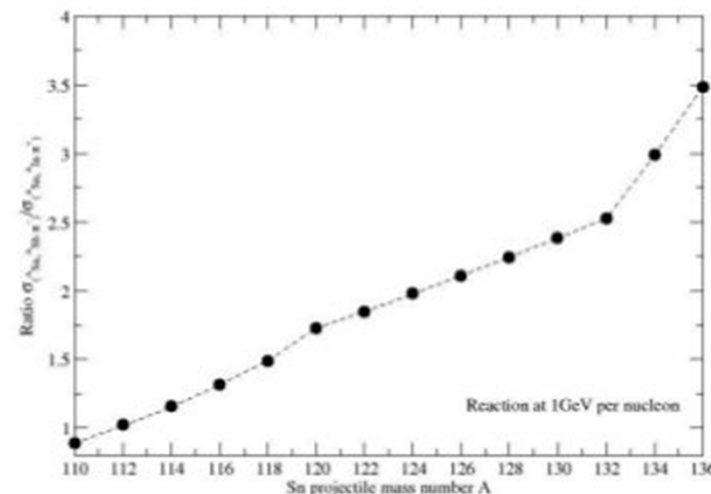
$$\cancel{n(p,\Delta^0)p} - \cancel{n(p,n\pi^0)p} \quad (2/3)$$

✓ hydrogen target

✓ pion tagging

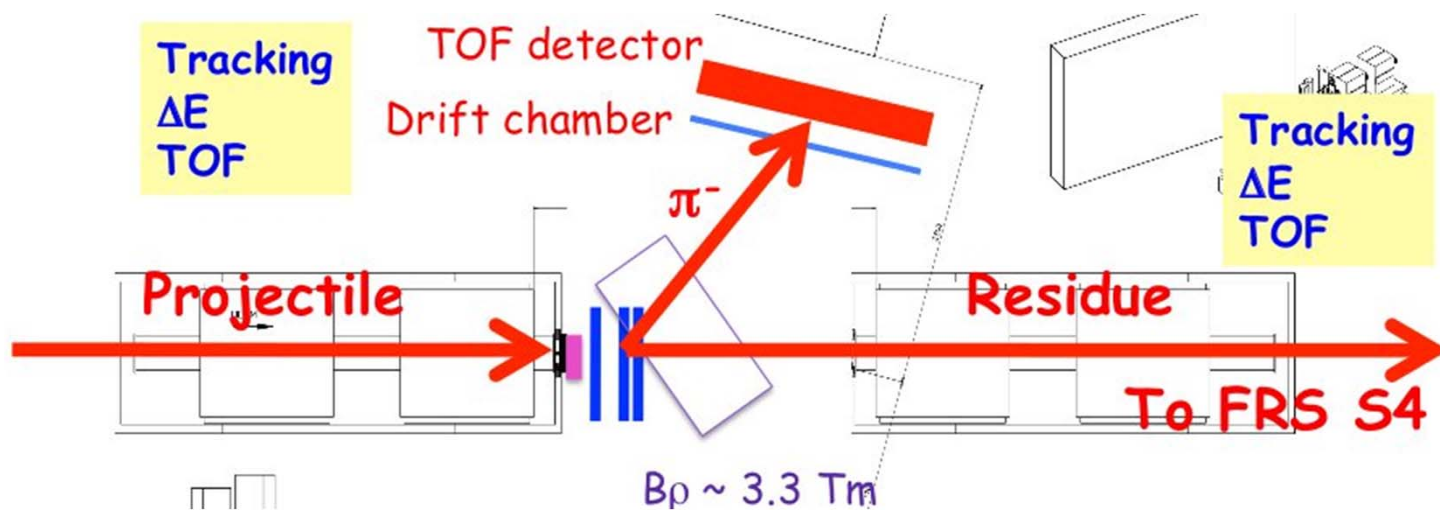
$$R_1 = \frac{\sigma_{np \rightarrow pp\pi^-}}{\sigma_{pp \rightarrow np\pi^+}} \frac{N_{np}}{N_{pp}} \sim \frac{\sigma_{np \rightarrow pp\pi^-}}{\sigma_{pp \rightarrow np\pi^+}} \frac{N_n^{(P)} N_p^{(T)}}{N_p^{(P)} N_p^{(T)}} = \frac{N_n^{(P)}}{N_p^{(P)}} \times \left(\frac{\sigma_{np \rightarrow pp\pi^-}}{\sigma_{pp \rightarrow np\pi^+}} \right)$$

Using a hydrogen target and tagging projectile pions, the ratio of the cross sections for both charge-exchange channels is proportional to the neutron/proton abundance at the periphery.



Next steps at GSI/FAIR

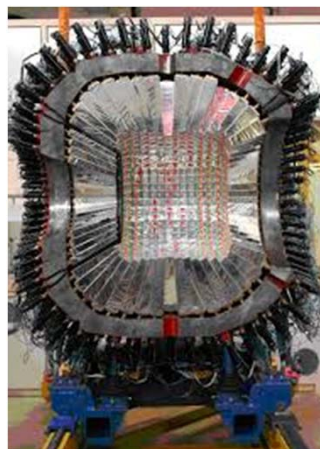
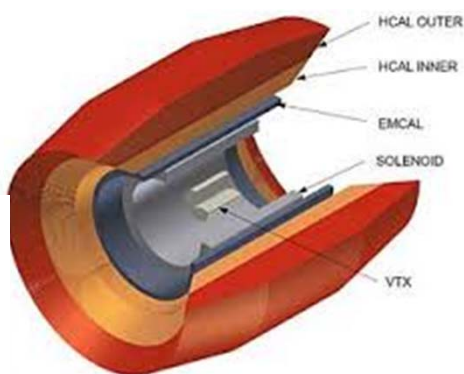
- ✓ A new experimental proposal for FAIR phase 0
 - improved momentum resolution with the FRS
 - liquid hydrogen target
 - exclusive measurements detecting projectile pions in coincidence



From T. Saito

Next steps at GSI/FAIR

- ✓ A new experimental proposal for FAIR phase 0
 - improved momentum resolution with the FRS
 - liquid hydrogen target
 - exclusive measurements detecting projectile pions in coincidence
- ✓ An experimental program for FAIR phase 1
 - larger acceptance and resolution at the SuperFRS
 - secondary beams: excitation of nucleon resonances in asymmetric nuclear matter
 - cylindrical detector (solenoid+tracking) for detecting projectile and target pions (WASA?)



Conclusions

- ✓ A high-resolving power magnetic spectrometer has been proven to be an excellent tool to identify nucleonic excitations in heavy-ion isobaric charge-exchange reactions:
 - several baryon resonances were identified in the projectile remnant missing-energy spectra
 - cross sections for elastic and inelastic, (p,n) and (n,p) reactions were also measured
 - in-medium properties of these baryons and the relative abundance of protons and neutrons at the nuclear periphery are being investigated using reliable model calculations

- ✓ The Super-FRS at FAIR will offer unique opportunities for these investigations:
 - extremely asymmetric nuclear matter
 - improved separation capabilities (pre-separator) and resolution
 - exclusive measurements detecting pions in coincidence
 - joint effort with the η' -nuclei and hypernuclei physics cases for the Super-FRS
 - unique physics case for FAIR

Collaborators

U. Santiago de Compostela: J.L. Rodríguez, J. Vargas, Y. Ayyad, S. Beceiro, D. Cortina, P. Díaz, M. Mostazo, C. Paradela

GSI: T. Aumann, J. Atkinson, K. Boretzky, A. Estrade, H. Geissel, A. Kelic, Y. Litvinov, S. Pietri, A. Prochazka, M. Takechi, C. Scheidenberger, H. Weick, J. Winfield

CEA/DAM: A. Chatillon, J. Taieb

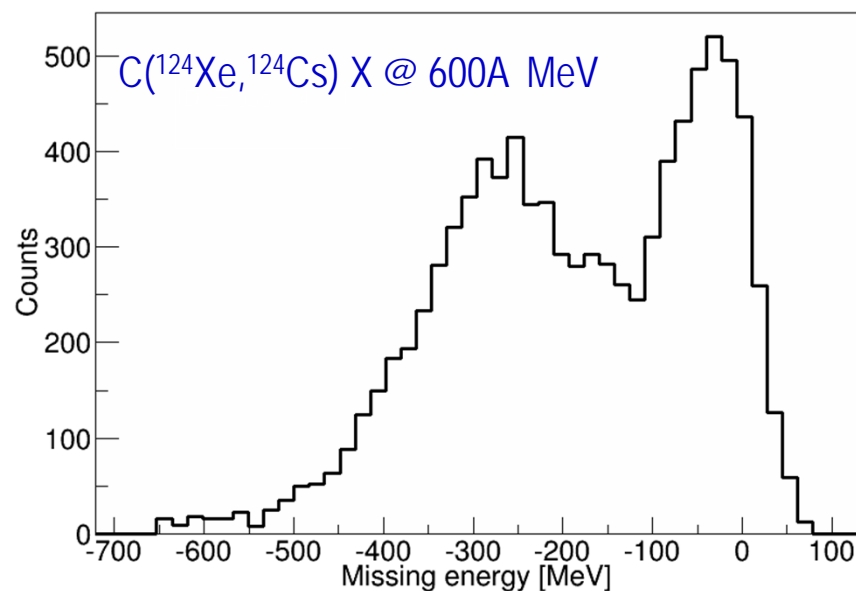
U. Coimbra: I. Vidaña

U. Giessen: H. Lenske

U. Beihang, RCNP : I. Tanihata

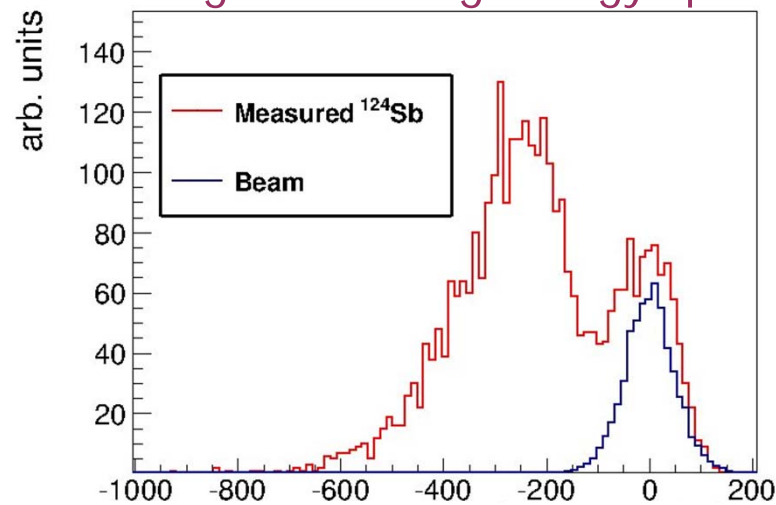
Next steps at GSI/FAIR

- ✓ A new experimental proposal at FRS@GSI
 - improved momentum resolution with the FRS



Recent measurements with the FRS

Unfolding the missing-energy spectrum with the experimental response function

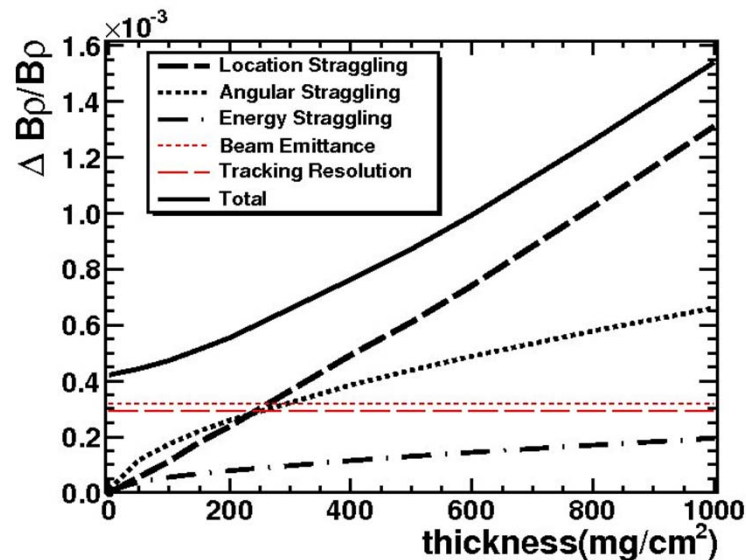


$$Y(i) = \sum_{j=1}^{n_{bin}} H(i-j) \cdot X(j)$$

Y: measured spectrum

H: experimental response function

X: observable



The primary beam centred through the FRS constitutes our response function H

Recent measurements with the FRS

Unfolding the missing-energy spectrum with the experimental response function

The most reliable unfolding techniques are based on iterative procedures (Richardson-Lucy)

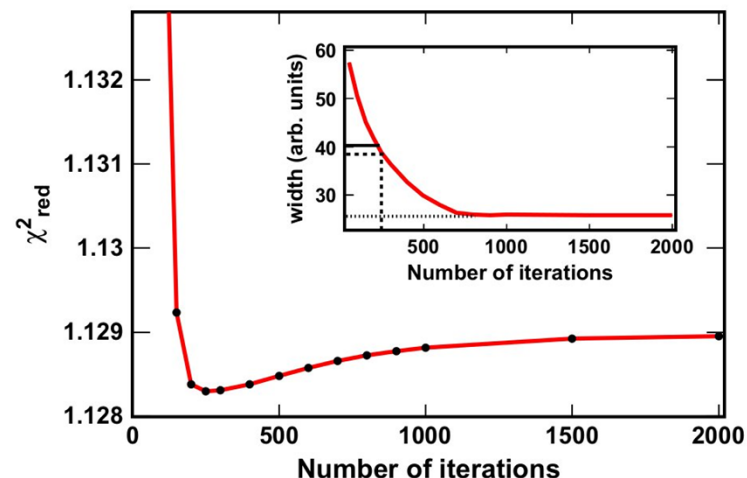
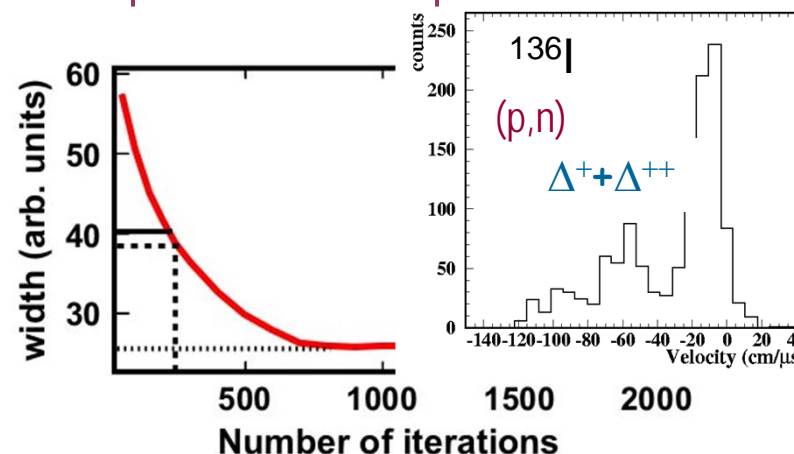
$$X^{(m)}(i) = X^{(m-1)}(i) \frac{\sum_{j=1}^{n_{bins}} H(j-i) \frac{Y(j)}{\sum_{k=1}^{n_{bin}} H(j-k) X^{(m-1)}(k)}}{\sum_{j=1}^{n_{bins}} H(j-i)}$$

A stopping condition is needed to determine the optimum number of iterations

$$Y^{Conv}(i) = \sum_{j=1}^{n_{bins}} H(i-j) \cdot X^{Calc}(j)$$

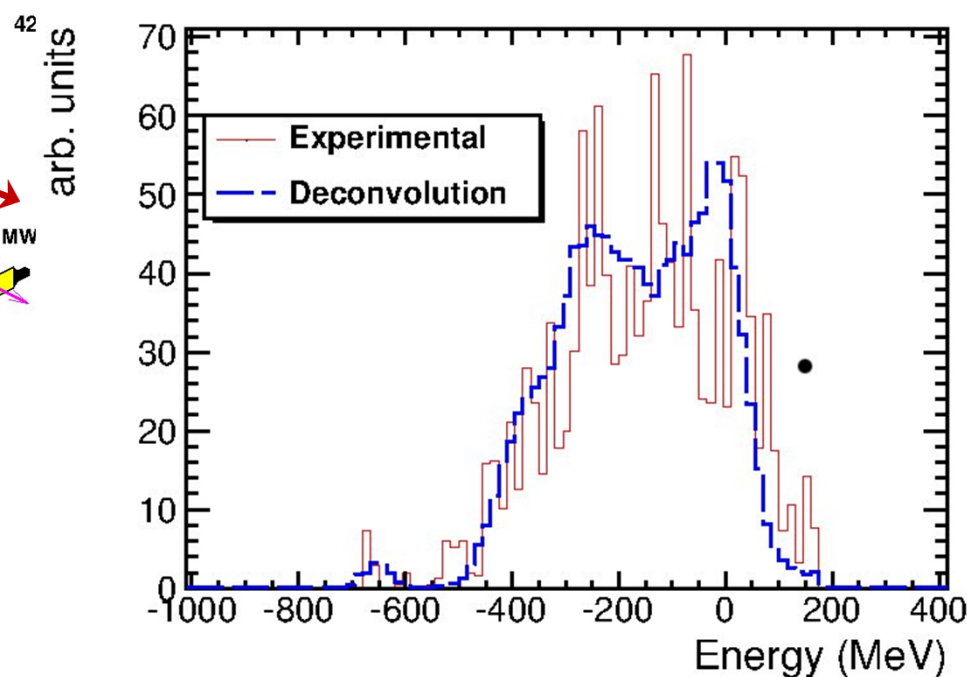
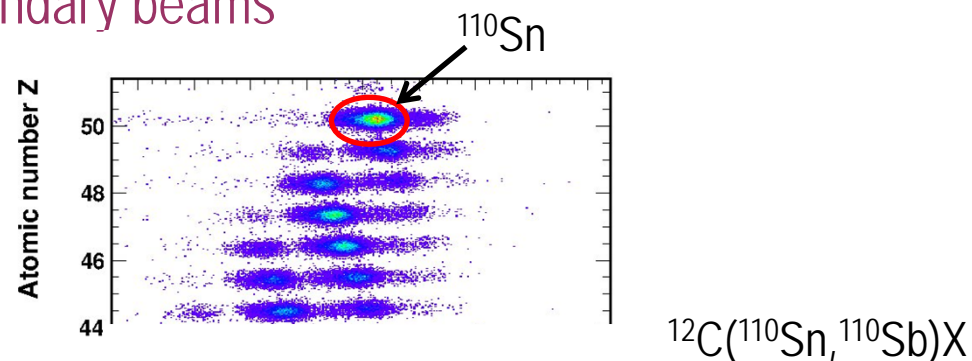
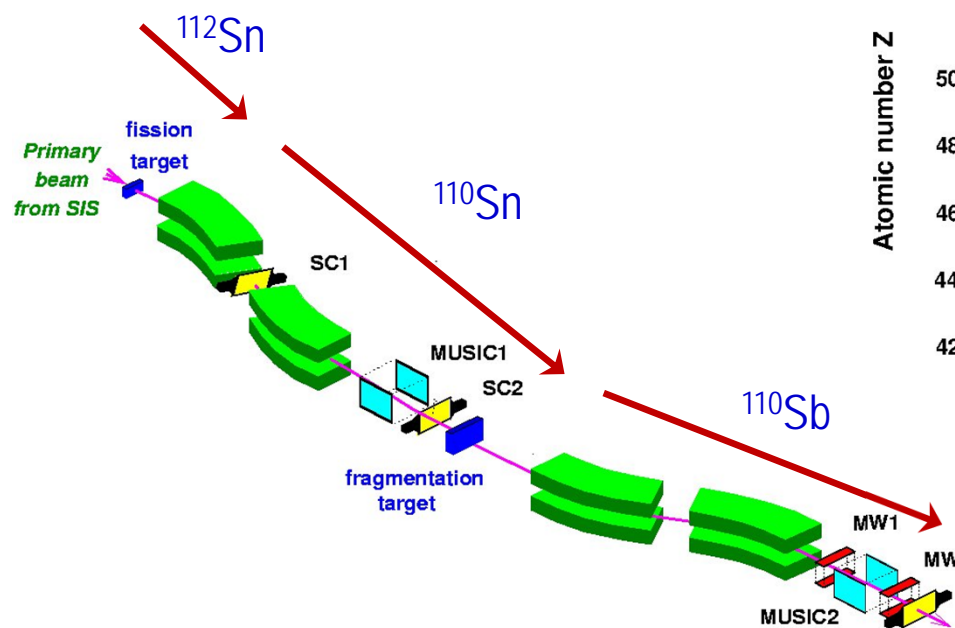
$$\chi_{red}^2 = \frac{1}{(n'-1)} \sum_{i=1}^{n_{bins}} \left(\frac{Y(i) - Y^{Conv}(i)}{\varepsilon(i)} \right)^2$$

J. Vargas, J.B. and M. Caamaño NIMA 707 (2013) 16



Recent measurements with the FRS

Missing-energy spectra with secondary beams



Main difficulties:

- Low statistics
- Thick S2 target ($1 \text{ g/cm}^2 \text{ C}$)
- Important background at S2

Options to isolate individual resonance excitations

Δ -resonance identification

(p,n)

$\Delta(1232)$ excitation	
excitation the target	excitation in the projectile
$p(p,n)\Delta^{++} = p(p,n)p\pi^+ \quad [\sqrt{2}]$	$p(p,\Delta^+)p = p(p,n\pi^+)p \quad [-\sqrt{2}/3]$
$n(p,n)\Delta^+ = n(p,n)n\pi^+ \quad [\sqrt{2}/3]$	$n(p,\Delta^+)n = n(p,n\pi^+)n \quad [\sqrt{2}/3]$
$n(p,n)\Delta^+ = n(p,n)p\pi^0 \quad [-2/3]$	$n(p,\Delta^0)p = n(p,n\pi^0)p \quad [2/3]$
$N^*(1440)$ excitation	
excitation in the target	excitation in the projectile
$n(p,n)P_{11}^+ = n(p,n)n\pi^+ \quad [-2\sqrt{2}]$	$p(p,P_{11}^+)p = p(p,n\pi^+)p \quad [-\sqrt{2}]$
$n(p,n)P_{11}^+ = n(p,n)p\pi^0 \quad [2]$	$n(p,P_{11}^+)n = n(p,n\pi^+)n \quad [\sqrt{2}]$
	$n(p,P_{11}^0)p = n(p,n\pi^0)p \quad [-2]$

(n,p)

$\Delta(1232)$ excitation	
excitation in the target	excitation in the projectile
$p(n,p)\Delta^0 = p(n,p)n\pi^0 \quad [2/3]$	$p(n,\Delta^0)p = p(n,p\pi^-)p \quad [-\sqrt{2}/3]$
$p(n,p)\Delta^0 = p(n,p)p\pi^- \quad [-\sqrt{2}/3]$	$p(n,\Delta^+)n = p(n,p\pi^0)n \quad [-2/3]$
$n(n,p)\Delta^- = n(n,p)n\pi^- \quad [-\sqrt{2}]$	$n(n,\Delta^0)n = n(n,p\pi^-)n \quad [\sqrt{2}/3]$
$N^*(1440)$ excitation	
excitation in the target	excitation in the projectile
$p(n,p)P_{11}^0 = p(n,p)n\pi^0 \quad [-2]$	$p(n,P_{11}^0)p = p(n,p\pi^-)p \quad [-\sqrt{2}]$
$p(n,p)P_{11}^0 = p(n,p)p\pi^- \quad [2\sqrt{2}]$	$p(n,P_{11}^+)n = p(n,p\pi^0)n \quad [2]$
	$n(n,P_{11}^0)n = n(n,p\pi^-)n \quad [\sqrt{2}]$

✓ Hydrogen target + 400 A MeV (only Δ excitation)

(n,p) + π^- detection $\rightarrow \Delta^0$ in projectile and target with similar probability ($\theta < 60^\circ$ more projectile than target)

(p,n) + π^+ detection $\rightarrow \Delta^{++}$ in target more probable than Δ^+ in projectile ($\theta > 90^\circ$ mostly target)

In both cases the background from quasi-elastic charge-exchange reactions is removed

Options to isolate individual resonance excitations

P_{11} -resonance identification

(p,n)

$\Delta(1232)$ excitation	
excitation the target	excitation in the projectile
$p(p,n)\Delta^{++} = p(p,n)p\pi^+ [\sqrt{2}]$	$p(p,\Delta^+)p = p(p,n\pi^+)p [-\sqrt{2}/3]$
$n(p,n)\Delta^+ = n(p,n)n\pi^+ [\sqrt{2}/3]$	$n(p,\Delta^+)n = n(p,n\pi^+)n [\sqrt{2}/3]$
$n(p,n)\Delta^+ = n(p,n)p\pi^0 [-2/3]$	$n(p,\Delta^0)p = n(p,n\pi^0)p [2/3]$
$N^*(1440)$ excitation	
excitation in the target	excitation in the projectile
$n(p,n)P_{11}^+ = n(p,n)n\pi^+ [-2\sqrt{2}]$	$p(p,P_{11}^+)p = p(p,n\pi^+)p [-\sqrt{2}]$
$n(p,n)P_{11}^+ = n(p,n)p\pi^0 [2]$	$n(p,P_{11}^+)n = n(p,n\pi^+)n [\sqrt{2}]$
	$n(p,P_{11}^0)p = n(p,n\pi^0)p [-2]$

(n,p)

$\Delta(1232)$ excitation	
excitation in the target	excitation in the projectile
$p(n,p)\Delta^0 = p(n,p)n\pi^0 [2/3]$	$p(n,\Delta^0)p = p(n,p\pi^-)p [-\sqrt{2}/3]$
$p(n,p)\Delta^0 = p(n,p)p\pi^- [-\sqrt{2}/3]$	$p(n,\Delta^+)n = p(n,p\pi^0)n [-2/3]$
$n(n,p)\Delta^- = n(n,p)n\pi^- [-\sqrt{2}]$	$n(n,\Delta^0)n = n(n,p\pi^-)n [\sqrt{2}/3]$
$N^*(1440)$ excitation	
excitation in the target	excitation in the projectile
$p(n,p)P_{11}^0 = p(n,p)n\pi^0 [-2]$	$p(n,P_{11}^0)p = p(n,p\pi^-)p [-\sqrt{2}]$
$p(n,p)P_{11}^0 = p(n,p)p\pi^- [2\sqrt{2}]$	$p(n,P_{11}^+)n = p(n,p\pi^0)n [2]$
	$n(n,P_{11}^0)n = n(n,p\pi^-)n [\sqrt{2}]$

✓ Hydrogen target + (p,n) channel + 700 A MeV (Δ and P_{11} excitation)

P^+ decay into $n+\pi^+\pi^0$ rejects any Δ excitation

$N(1440) \rightarrow N\pi$ 55 – 75%

$N(1440) \rightarrow N\pi\pi$ 30 – 40%

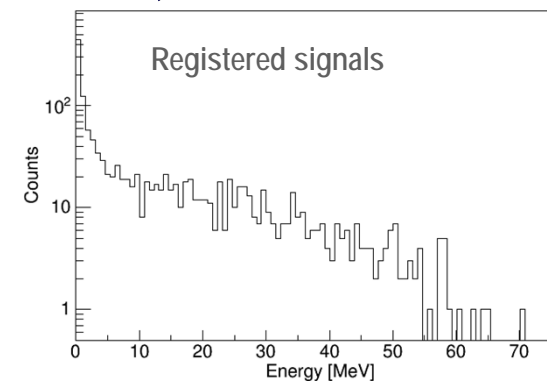
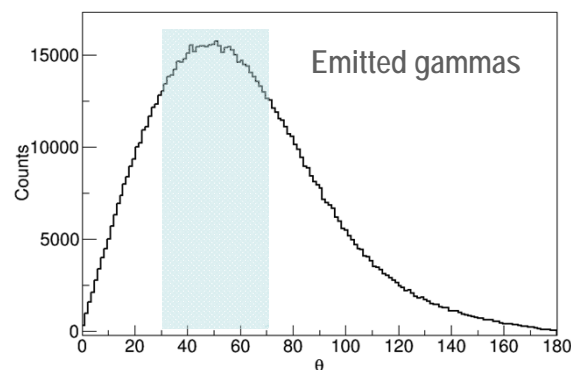
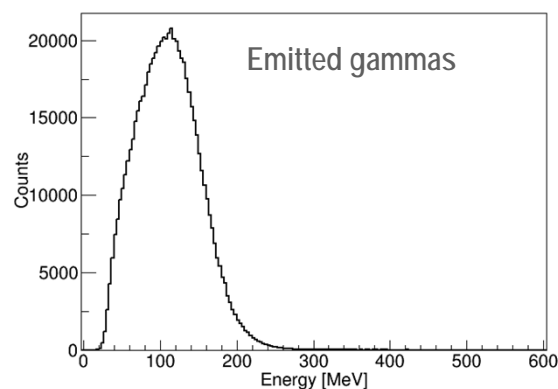
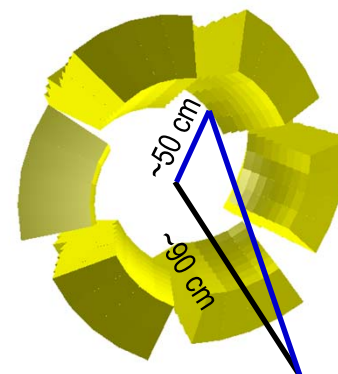
$P_{11}^+ \rightarrow n\pi^+\pi^0$

- π^0 decay into photons $\pi^0 \rightarrow \gamma\gamma$
- Measurement of the charged pion momentum \rightarrow shift in the total energy spectrum due to the π^0 .

Options to isolate individual resonance excitations

P_{11} -resonance identification from $\pi^0 \rightarrow \gamma\gamma$

Simulations with six CALIFA petals

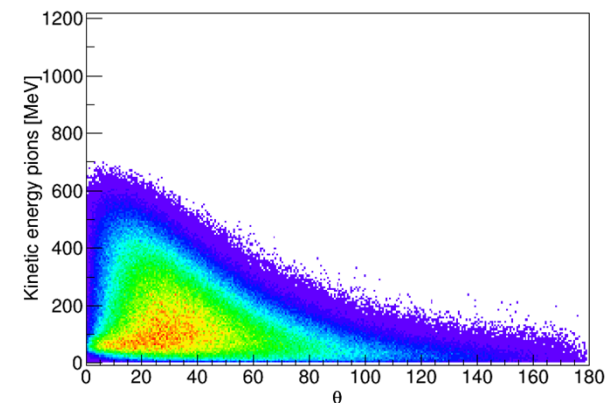
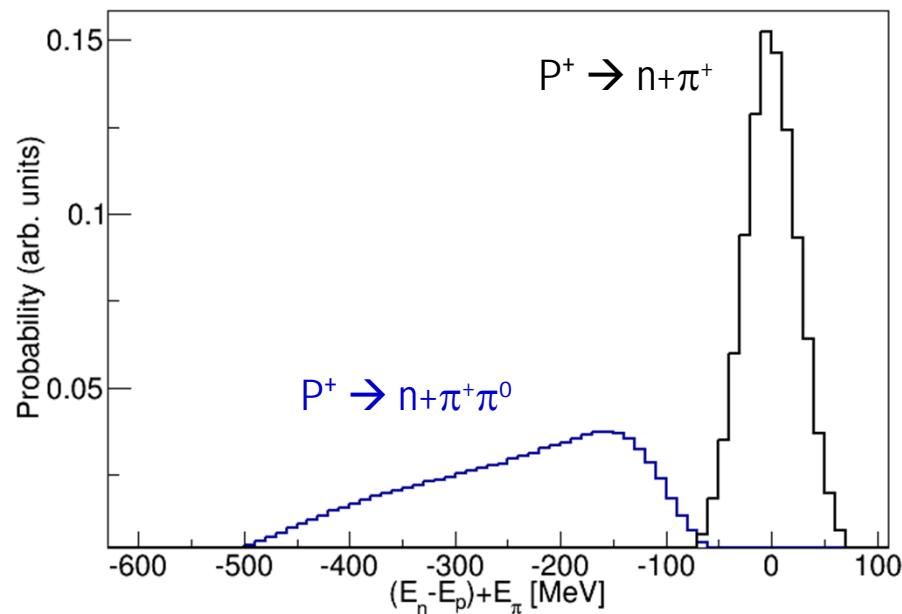


- ✓ Total efficiency for two simultaneous signals above 500 keV ~ 49% (42% above 1000 keV).
- ✓ Detailed simulations of the atomic background required.

Options to isolate individual resonance excitations

P_{11} -resonance identification from missing energy spectra in $P^+ \rightarrow n+\pi^+\pi^0$

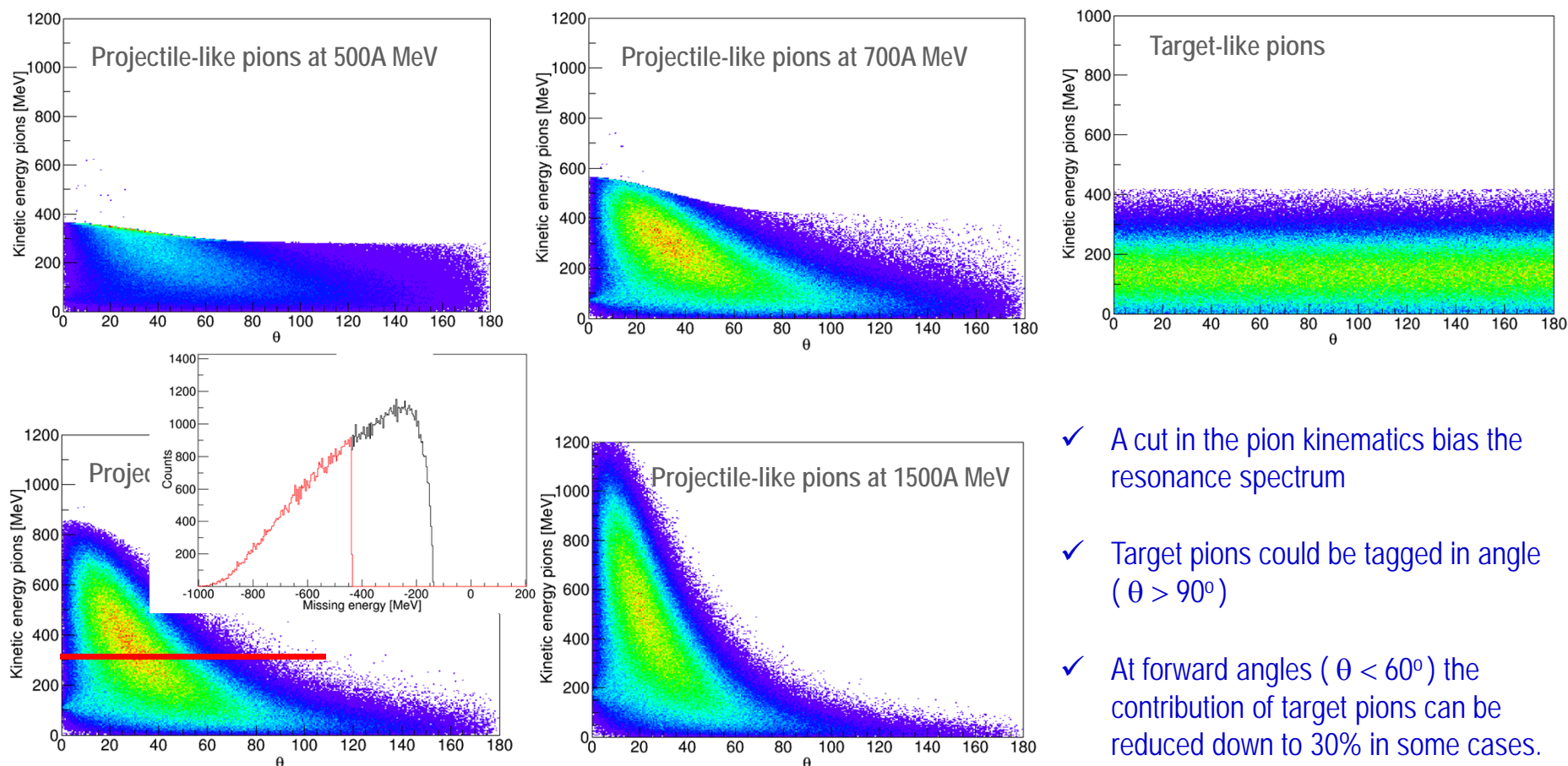
π^+ momentum measurement



- ✓ The estimated resolution for the pion momentum measurement $\sim 10\%$.
- ✓ Lowest possible threshold and relatively large angular range for pion detection.
- ✓ Detailed simulations with a specific pion detection setup to be done.

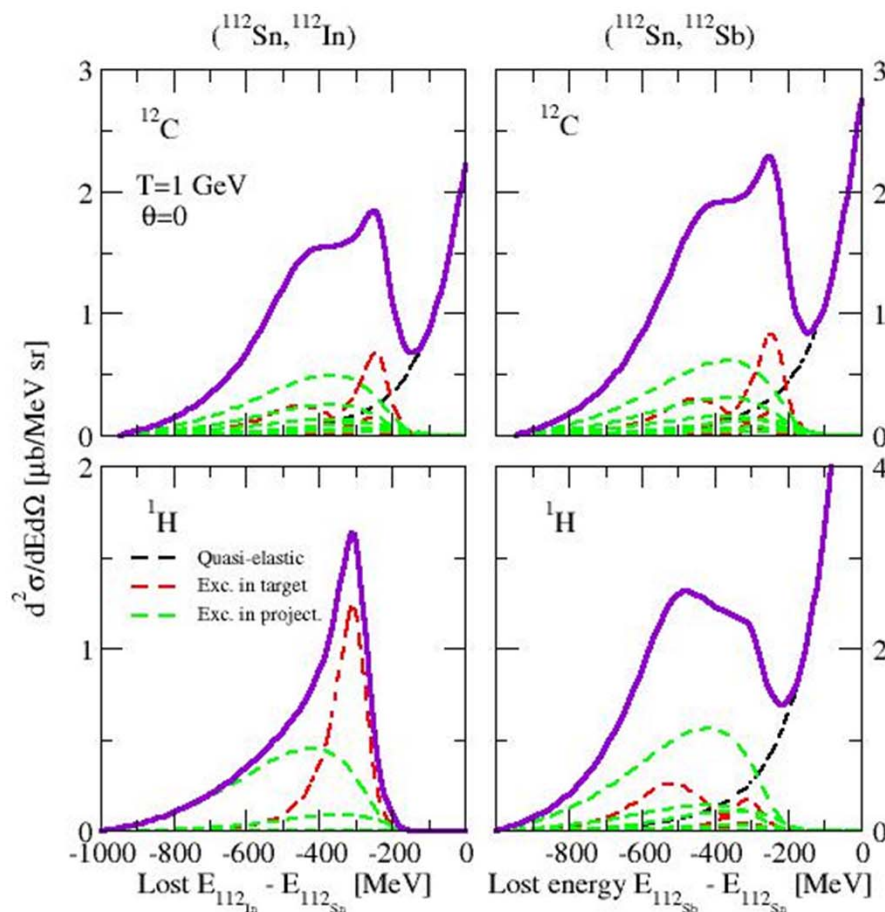
Options to isolate individual resonance excitations

Kinematical identification of projectile/target pions

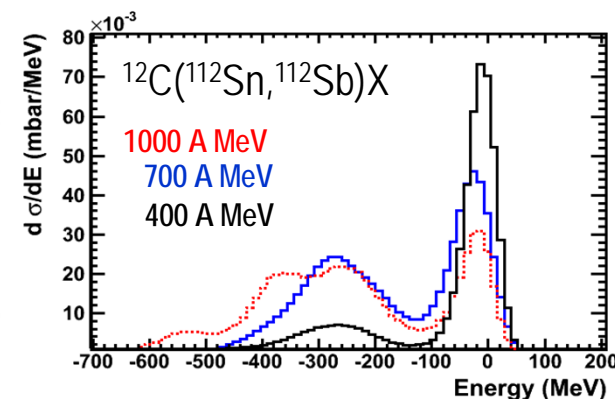


- ✓ A cut in the pion kinematics bias the resonance spectrum
- ✓ Target pions could be tagged in angle ($\theta > 90^\circ$)
- ✓ At forward angles ($\theta < 60^\circ$) the contribution of target pions can be reduced down to 30% in some cases.

Model calculations



Isaac Vidaña, U. Coimbra
Preliminary calculations



- ✓ Reactions induced on protons are the more selective to the excitation of the Delta and the Roper.
- ✓ Measurements at different energies can also be used to select the Delta and Roper in carbon